Optical wire-grid polarizers at oblique angles of incidence

X. J. Yu and H. S. Kwok[a)]
Center for Display Research, Department of Electrical and Electronic Engineering, Hong Kong University of Science and Technology, Clear Water Bay, Kowloon, Hong Kong

(Received 28 October 2002; accepted 20 January 2003)

Nanotechnology enables the fabrication of wire-grid polarizers (WGP) in the visible optical region. At oblique angles of incidence, WGP can be used as polarizing beam splitters (PBS). As such, they have the advantages of large numerical aperture and high-extinction ratios in both transmission and reflection. Because of these properties, WGP is being explored as PBS replacement in projectors. In this article, we present a complete theoretical investigation of the WGP. Rigorous diffraction theory, exact lowest-order eigenmode effective-media theory, and form birefringence theory are discussed. These theories are compared with experimental measurement of $T(\theta)$ and $R(\theta)$ as a function of the polarization state of the input light and as a function of the incident angle θ. It is shown that only the rigorous diffraction theory can fit the data for all incident angles. Using diffraction theory we provide a calculation relating the optical properties of the WGP to the physical dimensions of the wire grids. Thus, a framework for optimizing the optical properties of the WGP for various applications and requirements is provided. © *2003 American Institute of Physics.*
[DOI: 10.1063/1.1559937]

I. INTRODUCTION

Wire grid polarizers (WGP) have been used extensively in the infrared for a long time.[1] Various theories have been developed to model these polarizers. Recently, WGP have been successfully fabricated in the visible region using nanofabrication techniques.[2,3] At oblique angles of incidence, WGP can be used as polarizing beam splitters (PBS). PBS based on WGP has the potential advantages of wide bandwidth and large numerical aperture (NA). Thus such PBS are promising alternatives to conventional prism-type PBS for applications in projection displays. Recently, several experimental studies have been carried out to characterize these WGP.[3,4] In particular, we have recently performed a thorough investigation of the light utilization efficiency η and the extinction ratio ϵ of the WGP PBS as a function of the light incident angle.[4] Such angular dependence measurements are crucial in identifying the optimal operating conditions for the WGP when applied to projection applications, and have never been investigated systematically before. The angular dependence of η and ϵ are derived from the transmission and reflection coefficients $T(\theta)$ and $R(\theta)$ of the WGP for both *p*- and *s*- polarized lights.

Obviously, it is important to have a predictive theory of the WGP that relates $T(\theta)$ and $R(\theta)$ to the physical design such as width and depth of the grating. For example, it should be possible to fabricate devices with good reflection extinction ratios as well as transmission extinction ratios at a desired angle of incidence for projection applications. While WGP have been studied quite thoroughly, no systematic investigation of the angular dependence of $T(\theta)$ and $R(\theta)$ has been performed, let alone the fitting of the theory to such experimental angular dependence data. It is the purpose of this article to present a theory of the WGP, with special emphasis on fitting experimentally measured angular dependence of $T(\theta)$ and $R(\theta)$. We shall show that the rigorous diffraction theory can be used to fit all measured data very well. Approximate theories such as form birefringence do not agree with the experimental results as well, and can be quite wrong in some situations.

The most common explanation of the WGP is based on the restricted movement of electrons perpendicular to the metal wires.[1] If the incident wave is polarized along the wire direction, the conduction electrons are driven along the length of the wires with unrestricted movement. The physical response of the wire grid is essentially the same as that of a thin metal sheet. In the Ewald–Oseen picture, the coherently excited electrons generate a forward traveling as well as a backward traveling wave, with the forward traveling wave canceling exactly the incident wave in the forward direction. As a result, the incident wave is totally reflected and nothing is transmitted in the forward direction. An important observation that may affect the application of WGP is that a real current is generated on the metal surface. Free-carrier absorption due to phonon scattering is quite significant, if the mean free path of the electrons is smaller than the length of the wires, which is always the case. Thus joule heating occurs and energy is transferred from the electromagnetic field to the wire grid, in exactly the same manner as a metal sheet.[4,5]

In contrast, if the incident wave is polarized perpendicular to the wire grid, and if the wire spacing is wider than the wavelength, the Ewald–Oseen field generated by the electrons is not sufficiently strong to cancel the incoming field in the forward direction. Thus there is considerable transmission of the incident wave. The backward traveling wave is also much weaker leading to a small reflectance. Thus most of the incident light is transmitted. In form birefringence

a)Electronic mail: eekwok@ust.hk

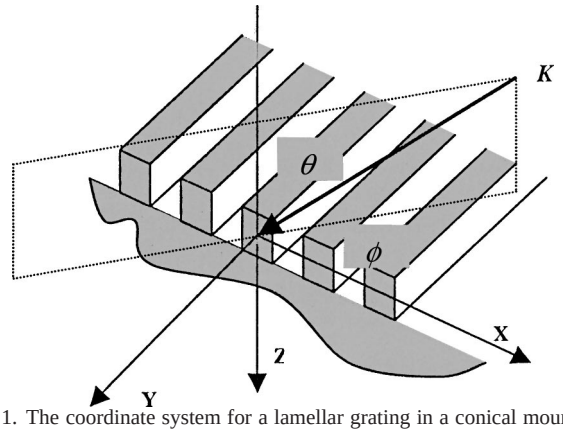

FIG. 1. The coordinate system for a lamellar grating in a conical mounting.

theory, the wire grid is said to behave as a dielectric rather than a metal sheet. Little energy is transferred from the field to the metal grid.

This is a useful qualitative explanation of the WGP. However, in actually trying to come up with a quantitative theory, it is necessary to invoke the rigorous theory of diffraction. We shall show that this theory can fit the experimental $T(\theta)$ and $R(\theta)$ data very well. We shall also show that the optimal design condition of the WGP mainly depends on $R(\theta)$. A Brewster angle can be defined for the WGP using $R(\theta)$. The relationship between $R(\theta)$ and the WGP physical parameters can be derived exactly, leading to further optimization of the WGP.

II. THEORETICAL ANALYSIS

A. Rigorous diffraction grating theory

A WGP in a conical configuration is shown in Fig. 1. The coordinate system is chosen such that the x axis is perpendicular to, and the y axis is parallel to the wire grid. The z axis is the normal to the overall structure. A plane wave is incident on the WGP at an arbitrary direction defined by the polar angle θ and a azimuthal angle ϕ. The metal wires are assumed to be rectangular in shape (lamellar) with a width of d_2 and a height of h. The distance between the grating wires is d_1. Thus the period of the grating is $d=d_1+d_2$. We can also define an aperture ratio (AR) of the grating as AR $=d_1/d$.

As a PBS, the WGP can have two possible configurations. The wires can either be perpendicular (structure S) and parallel (structure P) to the plane of incidence. They correspond to $\phi=0°$ and $\phi=90°$, respectively. Thus for the purpose of the present study, we do not consider arbitrary values of ϕ. Only θ is varied continuously. In this section, we shall calculate $T(\theta)$ and $R(\theta)$ for both structure S and structure P using rigorous diffraction grating theory.

The WGP are conducting lamellar gratings. Because the grating period is smaller than wavelength $(0.2<d/\lambda<0.5)$, zeroth-order grating theory is good enough for modeling the WGP. The rigorous diffraction theory has been applied by many authors in the past. Botten *et al.*[6–8] presented a series of papers on the analysis of lamellar gratings. However their analyses are limited to nonconical mountings ($\phi=0°$). Li presented a modal analysis of the WGP in arbitrary conical mountings in 1993.[9] This method has a much better convergence than the coupled-wave method.[10–12] We shall adopt this approach to analyze the WGP in the present paper. Structure S ($\phi=0°$) is exactly the same as the case analyzed by Botten *et al.* Structure P ($\phi=90°$) corresponds to a special case of conical mountings as discussed by Li.

We assume that the readers are familiar with the contents of Refs. 6–9. The discussion below will focus on the modifications of those papers for structures S and P of the WGP. The original Maxwell's equations can be represented by

$$\begin{pmatrix} \frac{\tilde{k}^2}{\varepsilon}\frac{\partial}{\partial x}\left(\frac{\varepsilon}{\tilde{k}^2}\frac{\partial}{\partial x}\right)+\frac{\partial^2}{\partial z^2}+\tilde{k}^2 & +\frac{k_y}{k_0}\frac{\tilde{k}^2}{\varepsilon}\left(\frac{d}{dx}\frac{1}{\tilde{k}^2}\right)\frac{\partial}{\partial z} \\ -\frac{k_y}{k_0}\frac{\tilde{k}^2}{\mu}\left(\frac{d}{dx}\frac{1}{\tilde{k}^2}\right)\frac{\partial}{\partial z} & \frac{\tilde{k}^2}{\mu}\frac{\partial}{\partial x}\left(\frac{\mu}{\tilde{k}^2}\frac{\partial}{\partial x}\right)+\frac{\partial^2}{\partial z^2}+\tilde{k}^2 \end{pmatrix} \times \begin{pmatrix} E_y \\ H_y \end{pmatrix}=0 \tag{1}$$

with the pseudoperiod conditions

$$\begin{aligned} E_y\left(\frac{d}{2},z\right)&=\exp(ik_xd)E_y\left(-\frac{d}{2},z\right),\\ H_y\left(\frac{d}{2},z\right)&=\exp(ik_xd)H_y\left(-\frac{d}{2},z\right),\\ \frac{\partial E_y}{\partial x}\left(\frac{d}{2},z\right)&=\exp(ik_xd)\frac{\partial E_y}{\partial x}\left(-\frac{d}{2},z\right),\\ \frac{\partial H_y}{\partial x}\left(\frac{d}{2},z\right)&=\exp(ik_xd)\frac{\partial H_y}{\partial x}\left(-\frac{d}{2},z\right), \end{aligned} \tag{2}$$

where

$$\tilde{k}^2=k^2(x)-k_y^2;\quad k_y=k_0\sin\theta\sin\phi;$$

$$k_x=k_0\sin\theta\cos\phi;\quad k_0=\frac{2\pi}{\lambda_0}n_0;\quad k(x)=n(x)k_0.$$

Solving these two equations, we can get the following equation:

$$\cos\gamma_1d_1\cos\gamma_2d_2-\frac{1}{2}\left(\frac{\sigma_2\gamma_1}{\sigma_1\gamma_2}+\frac{\sigma_1\gamma_2}{\sigma_2\gamma_1}\right)\sin\gamma_1d_1\sin\gamma_2d_2-\cos k_xd=0, \tag{3}$$

where for $j=1,2$, $\gamma_j^2=\tilde{k}_j^2-\rho$; $\sigma_i=n_i^2$ for TM *mode*, $\sigma_i=1$ for TE *mode*.

It should be noted that each possible modal field describing the variation of the field in the x direction is associated with a z component wave-vector ρ that is the solution of Eq. (3). For structure S, $\phi=0°$, Eq. (1) becomes the well-known Helmholtz equation. This is exactly what Botten *et al.* described in their papers. For structure P, $\phi=90°$, Eq. (1) shows that the electromagnetic fields are coupled. This has been solved by Li.[9] For our case of $\phi=90°$, a further simplification can be made. Letting $\phi=90°$, Eq. (3) can be factorized into the form

$$-\frac{2\sigma_1\sigma_2}{\gamma_1\gamma_2}\left[\frac{\gamma_1}{\sigma_1}\sin\left(\gamma_1\frac{d_1}{2}\right)\cos\left(\gamma_2\frac{d_2}{2}\right)+\frac{\gamma_2}{\sigma_2}\cos\left(\gamma_1\frac{d_1}{2}\right)\sin\left(\gamma_2\frac{d_2}{2}\right)\right]\left[\frac{\gamma_1}{\sigma_1}\cos\left(\gamma_1\frac{d_1}{2}\right)\sin\left(\gamma_2\frac{d_2}{2}\right)+\frac{\gamma_2}{\sigma_2}\sin\left(\gamma_1\frac{d_1}{2}\right)\cos\left(\gamma_2\frac{d_2}{2}\right)\right]=0. \tag{4}$$

The roots of these two factors are associated with, respectively, even and odd eigenfunctions of the electromagnetic field. It is similar to the normal incident case. The even and odd eigenfunctions can be solved and put into the form

$$U_e(x)=\begin{cases} C\cos\gamma_1 x & 0\leqslant|x|\leqslant\dfrac{d_1}{2} \\ C\left[\cos\dfrac{\gamma_1 d_1}{2}\cos\gamma_2\left(|x|-\dfrac{d_1}{2}\right)-\dfrac{\sigma_2\gamma_1}{\sigma_1\gamma_2}\sin\dfrac{\gamma_1 d_1}{2}\sin\gamma_2\left(|x|-\dfrac{d_1}{2}\right)\right] & \dfrac{d_1}{2}\leqslant|x|\leqslant\dfrac{d'}{2}\end{cases} \tag{5}$$

$$U_o(x)=\begin{cases} C\dfrac{1}{\gamma_1}\sin\gamma_1 x & 0\leqslant|x|\leqslant\dfrac{d_1}{2} \\ C\dfrac{1}{\gamma_1}\mathrm{sgn}(x)\left[\sin\dfrac{\gamma_1 d_1}{2}\cos\gamma_2\left(|x|-\dfrac{d_1}{2}\right)+\dfrac{\sigma_2\gamma_1}{\sigma_1\gamma_2}\cos\dfrac{\gamma_1 d_1}{2}\sin\gamma_2\left(|x|-\dfrac{d_1}{2}\right)\right] & \dfrac{d_1}{2}\leqslant|x|\leqslant\dfrac{d'}{2}\end{cases} \tag{6}$$

where C is a normalization constant. The eigenfunctions of the adjoint problem in this case can be obtained quite simply. It can be shown that

$$\overline{U^+(x)}=U(-x). \tag{7}$$

Once we get the eigenvalues from Eq. (3), we can calculate the complex amplitudes of the z component of the diffracted electric and magnetic fields. Finally, $T(\theta)$ and $R(\theta)$ of the gratings for different polarization can be calculated. The remaining procedures are the same as that presented in Li.[9]

It is crucial to obtain accurate eigenvalues from Eq. (3). Suratteau *et al.*[13] and Tayeb and Peht[14] provided an efficient, accurate numerical method to find these eigenvalues. But their solutions are limited to the Littrow condition, which is suitable for structure S but not for structure P. For the latter case, we need to modify that method further. We assume the readers are familiar with the contents of Ref. 14. The important change is that $\gamma_{1,2}$ is a function of θ and ρ as well. The results of the modifications are

$$G(\rho,t)=-\frac{\dfrac{\partial f}{\partial\theta}\dfrac{\partial\theta}{\partial t}+\dfrac{\partial f}{\partial\gamma_1}\dfrac{\partial\gamma_1}{\partial t}+\dfrac{\partial f}{\partial\gamma_2}\dfrac{\partial\gamma_2}{\partial t}+a\dfrac{\partial f}{\partial\varphi}\dfrac{\partial\varphi}{\partial t}}{\dfrac{\partial f}{\partial\gamma_1}\dfrac{\partial\gamma_1}{\partial\rho}+\dfrac{\partial f}{\partial\gamma_2}\dfrac{\partial\gamma_2}{\partial\rho}}, \tag{8}$$

where

$$\frac{\partial f}{\partial\theta}=-k_0 n_0 d\sin\{k_0 n_0 d\sin[\theta(t)]\cos\phi\}\cos\theta(t)\cos\phi;$$

$$\frac{\partial\gamma_1}{\partial t}=\frac{-\theta k_0^2\sin[2\theta(t)]\sin^2\phi}{2\gamma_1};$$

$$\frac{\partial\gamma_2}{\partial t}=\frac{k_0^2}{\gamma_2}(n_2-n_0)\varphi(t)-\frac{\theta k_0^2\sin[2\theta(t)]\sin^2\phi}{2\gamma_2} \tag{9}$$

$$\varphi(t)=1.5+(n_2-1.5)t$$

$$\theta(t)=\theta t\quad(0\leqslant t\leqslant 1)$$

$$\text{and}\quad a=\begin{cases}1 & \text{TM mode}\\ 0 & \text{TE mode.}\end{cases}$$

The definitions of the various terms are the same as in Ref. 14. Equations (1)–(9) are complete and can be solved to calculate the diffracted fields.

B. Exact lowest-order eigenmode effective-media theory and form birefringence theory

Haggans *et al.* presented an exact lowest-order eigenmode effective-media (ELOE EMT) theory to model zeroth-order gratings.[15] In their theory, the lamellar grating can be thought of as equivalent to one birefringence film. Based on Eq. (3), in the quasistatic limit $(d/\lambda\to 0)$ they get two equations

$$\frac{k_x^2}{n_0^2}+\frac{\rho^{(e)}+k_y^2}{n_0^2}=k_0^2;$$

$$\frac{k_x^2}{n_0^2}+\frac{\rho^{(h)}+k_y^2}{n_e^2}=k_0^2. \tag{10}$$

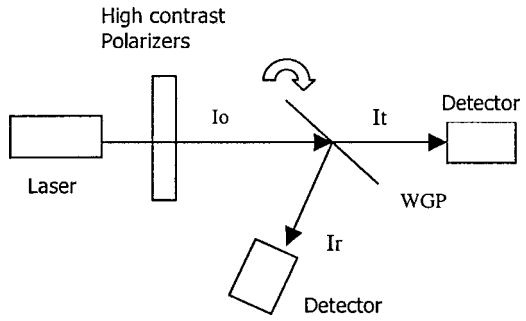

FIG. 2. Experimental arrangement.

These equations can also be obtained by expanding Eq. (3) in a Taylor series. Haggans *et al.* assumed that these two equations are also valid in the nonquasistatic limit. For different eigenvalues ρ, which depend on the incident angles θ and ϕ, the refractive index can be calculated. This theory is simple and powerful for modeling dielectric gratings. But for the metallic gratings, this approach was shown to be completely wrong in the nonquasistatic limit.[15] ELOE EMT cannot be applied to model the WGP.

However, Eq. (10), which is based on Eq. (3) in the quasistatic limit, can be used to derive a useful result

$$n_0^2 = n_1^2 \frac{d_1}{d} + n_2^2 \left(1 - \frac{d_1}{d}\right),$$
$$\frac{1}{n_e^2} = \frac{1}{n_1^2} \frac{d_1}{d} + \frac{1}{n_2^2} \left(1 - \frac{d_1}{d}\right). \tag{11}$$

This is precisely the lowest-order form birefringence theory. This form birefringence was recently used to analyze the WGP in the visible due to its simplicity.[2,3] We shall show that this model of the WGP is not quite accurate. In some cases, $T(\theta)$ and $R(\theta)$ derived using this form birefringence theory can be totally wrong. Additionally, it will be shown that the form birefringence method cannot give the correct relationship between the WGP physical parameters and the optical performance. Thus we believe that only the exact diffraction theory can work well for the WGP.

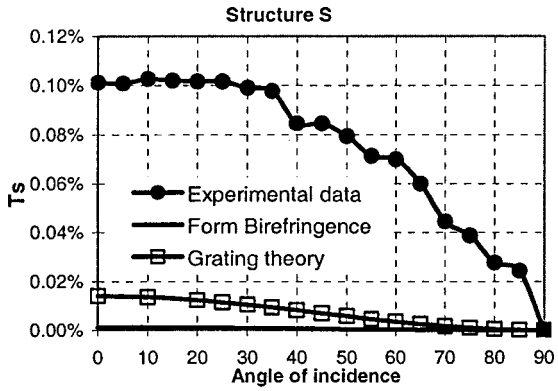

FIG. 4. T_s in structure S comparison between experimental data and simulation results.

III. COMPARISON WITH EXPERIMENTAL DATA

The WGP sample was obtained from Moxtek Inc., Orem, UT.[3] The transmission and reflectivity of the WGP in both structures S and P are measured as the function of the incident angle.[4] Details of that experiment as well as an interpretation of the data relevant to projection displays can be found in Ref. 4. Briefly, the experimental arrangement is shown in Fig. 2. Two high-contrast polarizers are used to filter the output of the green HeNe at a wavelength of 543.5 nm. The purity of the polarized light used in the measurement is better than 10^6. The same detector is used to measure the original light intensity I_o, and the reflected (I_r) and transmitted light (I_t). It was made sure that the distance from the detector to the laser was always the same, so that the absolute transmittance and reflectance could be obtained simply by dividing the signals as $T=I_t/I_o$, and $R=I_r/I_o$. By rotating the high-contrast polarizers, either *p* light or *s* light can be obtained. Thus the transmittance and reflectance of the WGP in either S or P geometry can be measured as a function of the incident angle θ.

For structure S, the WGP transmits *p* light and reflects *s* light. Experimentally, one can measure $T_p(\theta)$, $R_p(\theta)$, $T_s(\theta)$, and $R_s(\theta)$. Figures 3–6 show a comparison of the measured results and the rigorous diffraction grating theory as well as the simpler form birefringence theory. The fitting parameters were the period *d*, the height of the wires *h*, and

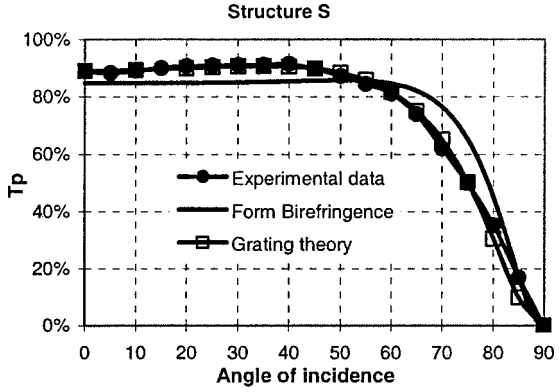

FIG. 3. T_p in structure S comparison between experimental data and simulation results.

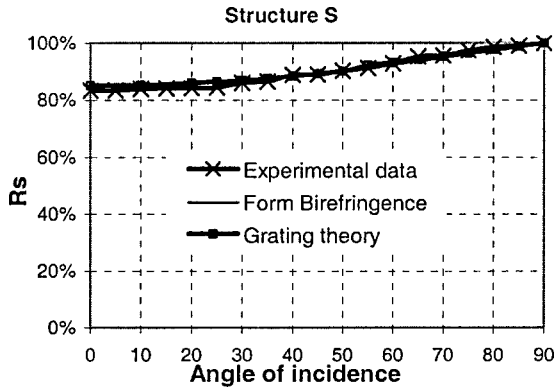

FIG. 5. R_s in structure S comparison between experimental data and simulation results.

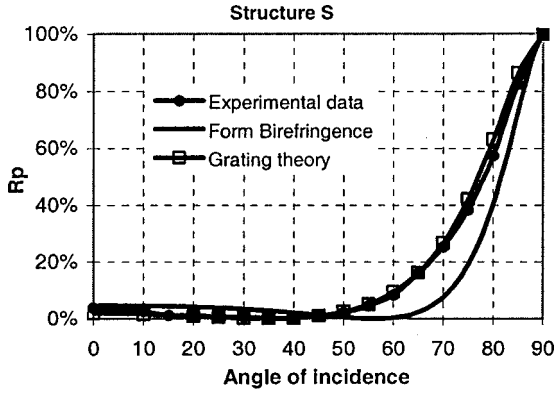

FIG. 6. R_p in structure S comparison between experimental data and simulation results.

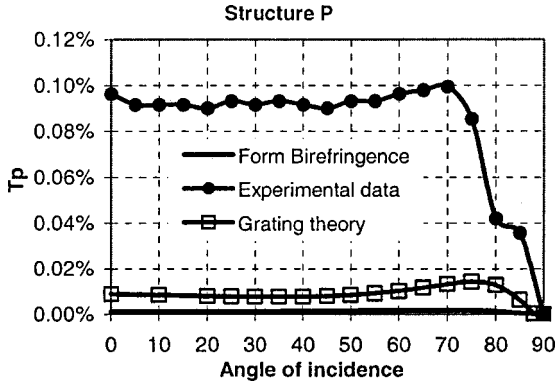

FIG. 8. T_p in structure P comparison between experimental data and simulation results.

the aperture ratio ($\mathrm{AR}=d_1/d$) of the WGP. The fitted results were 150 nm, 180 nm, and 0.55, respectively. These are in very good agreement with values supplied by the manufacturer. We have confirmed that the grating period is indeed 150 nm using a scanning electron microscope. The height of 180 nm and the aperture ratio of 0.55 are within the range of values given by the manufacturer.

In general, it can be seen that the fitting is excellent for the exact diffraction theory. For form birefringence theory, the deviation from the experimental results is small if the incident wave is polarized along the direction of the wire grids. This is the case in Fig. 5. But if the incident wave is polarized perpendicular to the wire grids, the predictions using form birefringence theory is quite inaccurate. This is the case for Figs. 3 and 6. In Fig. 4, it is seen that both diffraction and form birefringence theories are not in good agreement with the measured data. This is because the measured transmittance T_s is very small ($<0.15\%$) and there is a big experimental uncertainty. However, the disagreement between theory and experiment is insignificant in absolute terms.

As discussed in Ref. 4, and as can be seen from the measured data in Figs. 3–6, the transmission extinction ratio T_p/T_s has only weak angular dependence. On the other hand, the reflection extinction ratio R_s/R_p has a very strong angular dependence. These angular dependences affect directly the NA of the PBS. Hence the optimal operating condition of the WGP PBS depends mainly on $R_p(\theta)$. In Fig. 6 it can be seen that the behavior of $R_p(\theta)$ is similar to that of the Fresnel reflection of light by a dielectric, exhibiting a strong minimum at the Brewster angle. Therefore we shall define the minimum angle in $R_p(\theta)$ as the equivalent Brewster angle (θ_B) of the WGP. At this angle the WGP will have the highest-reflection extinction ratio. Interestingly, for the WGP, θ_B depends on the physical dimensions and orientation of the wire grid. It may actually be varied from 0 to 90° by choosing the dimension such as the height and width of the wire grid properly. For PBS applications, it is perhaps useful for the optimal angle of incidence to be at 45°.

For structure P, the WGP transmits *s* light and reflects *p* light. A similar set of experimental data can be obtained and compared with theoretical predictions. The results are shown in Figs. 7–10. Again it can be seen that the rigorous grating theory provides an excellent fit to all the experimental data. The form birefringence theory shows agreement if the light is polarized along the wires and shows great discrepancies if the wires are perpendicular to the light polarization. Similar to Fig. 4, the experimental data in Fig. 8 has very small values and large uncertainty. Here again, both theories do not agree well with the experimental data. Nevertheless the rigorous grating theory is in better agreement than the form birefringence theory. Also, similar to structure S, there is a minimum in the reflectance of R_p. This is the equivalent Brewster angle of the WGP for this geometry. The P struc-

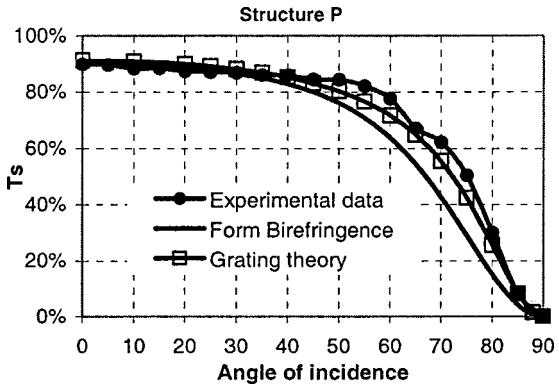

FIG. 7. T_s in structure P comparison between experimental data and simulation results.

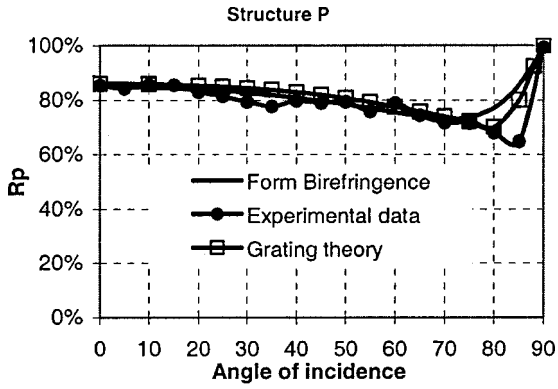

FIG. 9. R_p in structure P comparison between experimental data and simulation results.

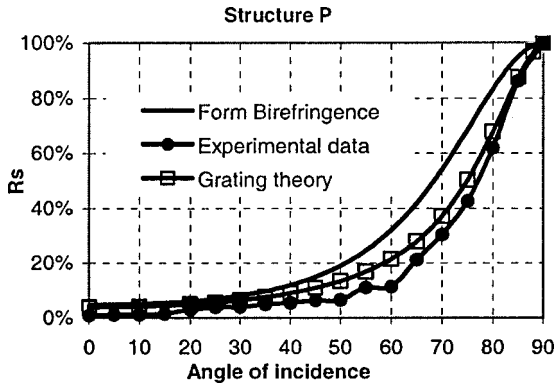

FIG. 10. R_s in structure P comparison between experimental data and simulation results.

ture Brewster angle is not the same as the one for the S structure, for obvious reasons. The positions of the wire grids are different. Actually for structure P, the minimum in R_p is quite mild and it is not too useful to talk about the Brewster angle in this case.

From the comparison above, it is concluded that the zeroth-order grating theory is the best method that can model the WGP well. Form birefringence, while simple and elegant, is not a good theory for the WGP.

IV. CONCLUSIONS

In this article, we have shown various ways of modeling the optical properties of the WGP. Extensive comparison with experimental data was also performed. The rigorous diffraction grating theory is shown to fit the experimental data very well. The form birefringence theory gives predicted extinction ratios that are orders of magnitude larger than those measured experimentally. It should be used with great care, even though it is an elegant approximation to the physics of the wire-grid polarizer.

The exact diffraction theory can be used in the design and analysis of the WGP. Using this theory we can calculate systematically the extinction ratio of the WGP as a function of the physical parameters such as grid spacing and height. A parameter space can be obtained showing the interdependence of the various optical properties such as absorption and extinction ratios. Such calculations can be very useful for the design of the WGP.

From the measured and calculated data of R_p for both the S and P structures, a minimum in reflection is observed. This minimum can be regarded as the equivalence to Brewster reflection in dielectrics. We defined that minimum as the equivalent Brewster angle for the WGP. This Brewster angle also depends on the physical dimensions and orientations of the wire grids. This equivalent Brewster angle is actually quite useful in analyzing and optimizing the extinction ratio of the WGP. One can optimize the physical dimension of the wire grids in order to achieve the best transmission throughput and highest-extinction ratio. This analysis will be the subject of a future publication.

ACKNOWLEDGMENTS

This research was supported by the Hong Kong Government Innovation and Technology Fund. We also thank Moxtek Inc, for supplying the WGP sample.

[1] E. Hecht, *Optics*, 3rd ed. (Addison-Wesley Longman, New York, 1998), pp. 327–328.
[2] T. Sergan, J. Kelly, M. Lavrentovich, E. Gardner, D. Hansen, R. Perkins, J. Hansen, and R. Critchfield, *Twisted Nematic Reflective Display with Internal Wire Grid Polarizer* (Society for Information Display, Boston, MA, 2002), pp. 514–517.
[3] Douglas Hansen, Eric Gardner, Raymond Perkins, Michael Lines, and Arthur Robbins, *Invited Paper: The Display Applications and Physics of the ProFlux™ Wire Grid Polarizer* (Society for Information Display, Boston, MA, 2002), pp. 730–733.
[4] X. J. Yu and H. S. Kwok, (unpublished).
[5] N. N. Rao, *Elements of Engineering Electromagnetics*, 5th ed. (Prentice-Hall, Englewood Cliffs, N.J., 2000).
[6] L. C. Botten, M. S. Craig, R. C. McPhedran, J. L. Adams, and J. R. Andrewartha, Opt. Acta **28**, 413 (1981).
[7] L. C. Botten, M. S. Craig, R. C. McPhedran, J. L. Adams, and J. R. Andrewartha, Opt. Acta **28**, 1087 (1981).
[8] L. C. Botten, M. S. Craig, and R. C. McPhedran, Opt. Acta **28**, 1103 (1981).
[9] L. Li, J. Mod. Opt. **40**, 553 (1993).
[10] M. G. Moharam and T. K. Gaylord, J. Opt. Soc. Am. **73**, 1105 (1983).
[11] M. G. Moharam and T. K. Gaylord, J. Opt. Soc. Am. **72**, 1385 (1982).
[12] C. W. Haggans and R. K. Kostuk, in *Optical Data Storage '91*, edited by J. J. Burke, N. Imamura, and T. A. Shull (Proceeding of the Society of Photo-optical Instrumentation Engineers, Vol. 1499, Colorado Springs, CO, 1991), pp. 293–302.
[13] J. Y. Suratteau, M. Cadilhac, and R. Petit, J. Opt. (Paris) **14**, 273 (1983).
[14] G. Tayeb and R. Petit, Opt. Acta **31**, 1361 (1984).
[15] C. W. Haggans, L. Li, and R. K. Kostuk, J. Opt. Soc. Am. A **10**, 2217 (1993).